

Energy absorption capabilities of complex thin walled structures

F Tarlochan*, Sami AlKhatib

Department of Mechanical and Industrial Engineering, Qatar Transportation and Traffic Safety Center (QTTSC), Qatar University, Doha, Qatar

* corresponding author: faris.tarlochan@qu.edu.qa

Abstract. Thin walled structures have been used in the area of energy absorption during an event of a crash. A lot of work has been done on tubular structures. Due to limitation of manufacturing process, complex geometries were dismissed as potential solutions. With the advancement in metal additive manufacturing, complex geometries can be realized. As a motivation, the objective of this study is to investigate computationally the crash performance of complex tubular structures. Five designs were considered. It was found that complex geometries have better crashworthiness performance than standard tubular structures used currently.

1. Introduction

The demand for new automotive vehicles is increasing yearly with the increase of world's population. According to the International Energy Agency number of automobile vehicles is expected to reach 1.7 billion by 2035 [1]. With the increase in number of vehicles on road, an increase in the number of car accidents is observed. According to the World Health Organization (WHO) the total number of road traffic deaths remains unacceptably high at 1.2 million per year. From this value, nearly 50% are vehicle occupants [2]. Automotive engineers play a major role in tackling this issue by ensuring the maximum level of safety for occupants when designing the automobile vehicles. This is achievable through passive safety measures where the vehicle's structure is designed to provide higher level of protection and safety in any crash event.

The main vehicle's structures responsible for crash energy absorption in frontal impacts are the frontal longitudinal members, alternatively called side members (See Figure 1). The side member is a thin-walled hollow tubular structure of rectangular or square cross section that dissipates crash energy through plastic deformation. Thin-walled structures are most widely used for crashworthiness and energy absorption applications, due to their light weight and high energy absorption efficiency [3]. Stringent automotive safety standards have driven engineers to enhance the energy absorption capacity without compromising on the overall vehicle weight. Numerous studies have been published on investigating energy absorption of metal tubular thin-walled structures. These studies can be categorized as follows: (1) studying the effect of different geometries and configurations and (2) investigating the effect of foam fillers.

A lot of work looking into different geometrical modifications and configurations of tube thickness designs have been carried out to enhance the energy absorption of thin-walled tubes. Most of the published work in this area looked at simple tubular designs which can be achieved with conventional manufacturing techniques. One of these modifications is dividing the thin-walled column into simple extruded multi-cells profiles that can fill the tube partially or fully. Tang et al [4] studied the



characteristics of multi-cells cylindrical tubes on energy absorption and found that multi-cell geometries enhance the energy absorption. Other work on multi-cells geometries studied the effect of different thin-walled tubes cross sections on energy absorption [5]. Varying the tubular structure thickness was another investigated geometrical alteration by researchers to enhance energy absorption and reduce weight [6, 7]. As well, the effect of varying the thickness of multi-cells tubular structures was studied [8]. Tailor made tubular structures were also studied as potential energy absorbers with varying thickness [9]. Expanded metal tubes were another approach taken by researchers to enhance the energy absorption and reduce weight of thin-walled structures [10 – 11]. Other researchers studied the effect of multi-cornered tubular structures on energy absorption [12, 13, and 14], while others investigated the energy characteristics of bi-tubular tubes [15] and nested tubular systems [16].

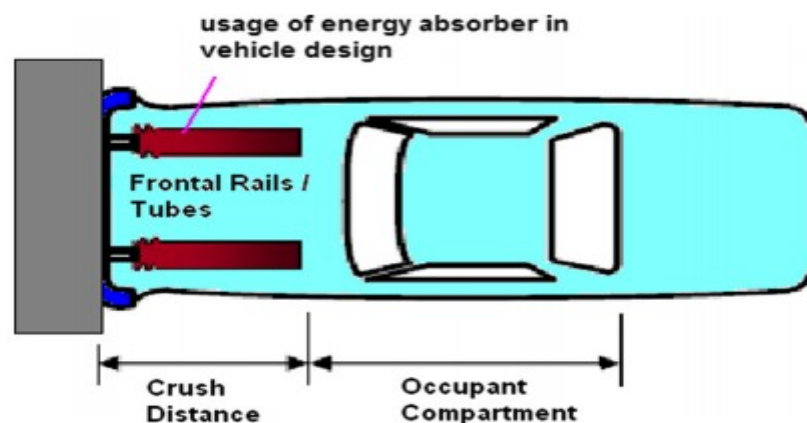


Figure 1. Frontal longitudinal thin-walled structures of the vehicle [3].

Other investigators looked into the effect of metal foam fillers into tubes. Because of its low initial stress peaks and extended load plateaus, foam is considered as an attractive energy absorber. Arriving to the perfect combination of foam and tubular structure requires the consideration of foam density, column width, thickness and cross-section profile and material properties. Some researchers looked into uniform foam density [17-25] fillers, while others looked into functionally graded foams [26-30]. In principle it was found that foams enhance crashworthiness performances, in particular functionally graded foams, if designed correctly.

The aforementioned solutions are limited to the available manufacturing techniques commonly used in producing thin-walled structures. Even the most recent studies in the area of crashworthiness applications are still focused on simple geometries. With the advancement in metal additive manufacturing (AM) it is now possible to produce complex geometries that can be integrated to the thin-walled structures. With this in mind, the main objective of the present work is to study numerically the energy absorption performance of complex thin walled structure geometries. This numerical study is the preliminary study to assess the capabilities of complex geometries in absorbing energy. The subsequent future step in this research framework is additively manufacture the best design selected numerically and to conduct dynamic crush test to actually assess the potential of such complex thin walled structures for energy absorption applications.

2. Performance indicators

The performance of the structures is mainly evaluated based on the overall crash response and based on the ease of manufacturing secondary. To assess the crash response the following parameters were consider.

2.1. Peak load

The peak load is the maximum load needed to start deforming the structure permanently. This parameter is of importance as it is the highest load felt by the occupant during the crash.

2.2. Energy absorption

The total energy absorption E in a crash equals the area under the load-displacement curve. It is defined as:

$$E = \int_0^{d_{max}} F ds \quad (1)$$

To relate how much energy a structure can absorb to its mass, specific energy absorption is obtained. It is defined as:

$$SEA = \frac{E}{m} \quad (2)$$

where m is the crushed mass of the structure. The SEA is very important to automotive industry where weight reduction is crucial.

2.3. Crush Force Efficiency (CFE)

The crushing force efficiency (CFE) is the ratio between the mean and peak crushing forces, the two parameters that are directly related to the deceleration level felt by the occupants. It is defined as:

$$CFE = \frac{P_{mean}}{P_{max}} \quad (3)$$

An ideal energy absorber would have a CFE value close to 100%. That is because an ideal absorber would preserve a peak load for its entire crushed length. If the CFE value is far from 100%, this indicates a large deceleration shift which will be dangerous for the passenger. To summarize, a good design would have a reasonable peak load, a high specific energy absorption, and a CFE value close to 100%.

3. Design methodology

This work aims to investigate the effect of complex geometries and structures on the crashworthiness characteristics of thin-walled tubular structures. To achieve this aim, five different complex designs were generated for numerical crash tests as shown in Figures 2 - 6. Each design has two different parameters that were altered to result in 4 profiles for each design. This was done to investigate the effect of each parameter on the crashworthiness performance indicators. Two materials were used to model the generated profiles, steel and aluminum. This was done to examine the effect of the material on the crash response of each profile. Each design's parameters and profiles are listed in Table 1. The numerical simulation includes an axial impact using a striker of 275 kg mass with an initial velocity of 15.6 m/s. The numerical modeling values are discussed in details in the next section. All of the design's profiles are thin-walled tubes with a cross-sectional area of 80x80 mm and a thickness of 2 mm. These dimensions were selected based on the average sedan car side member's dimensions. From the generated profiles, one profile was chosen via a multi-criteria decision making process.

For the multi-criteria decision making process, the first step is choosing the performance criteria. Two categories of performance criteria were considered. The main category includes the performance indicators discussed previously, while the other includes the level of ease of manufacturing. After choosing the performance criteria, the weightage of each criterion is formulated using the Digital Logic (DL) method [31]. In this method, comparison is made between only two performance criteria at a time. An example of determining the relative importance of each performance criterion is shown in Table 2, where a numerical value of (3) is given to the important criterion, and a numerical value of (1) is given for the less important criterion. If the two criteria are equally important, they are both given the numerical value of (2). Total number of possible comparisons can be determined by the following equation:

$$N = \frac{n(n-1)}{2} \quad (4)$$

where n is the number of performance criteria.

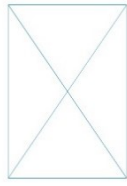
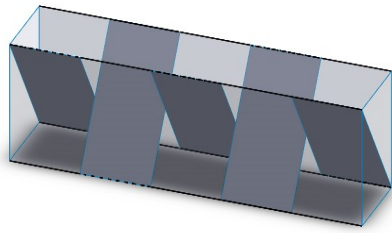


Figure 2. X-shaped internal plates.

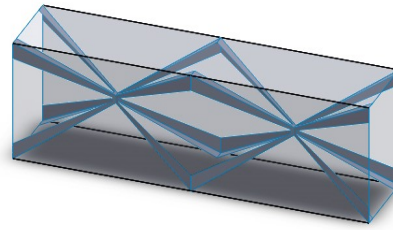


Figure 3. Pyramid's internal shapes.

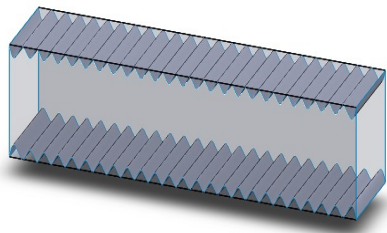


Figure 4. Wavy internal sheets.

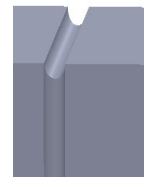
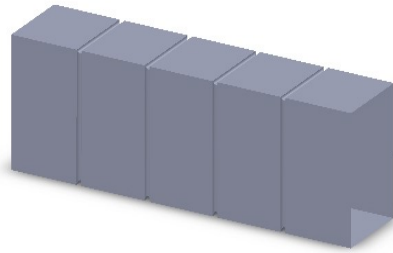


Figure 5. Circular surface grooves.

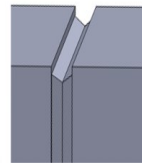
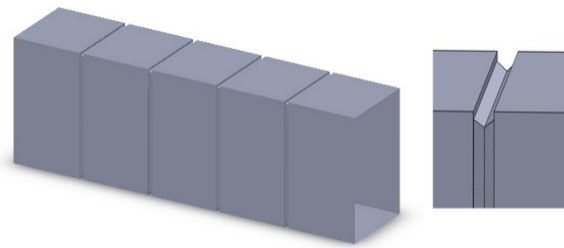


Figure 6. Hexagonal surface grooves.

Table 1. Design's parameters and abbreviations.

Design	Parameters	Abbreviation
Circular Grooves	Grooves Number=4, depth=5mm	CG4D5
	Number=6, D=5mm	CG6D5
	Number=4, D=7mm	CG4D7
	Number=6, D=7mm	CG6D7
Hexagonal Grooves	Grooves Number=4, depth=5mm	HG4D5
	Number=6, D=5mm	HG6D5
	Number=4, D=7mm	HG4D7
	Number=6, D=7mm	HG6D7
Pyramids	Pyramids Number=4, Thickness=1mm	P4T1
	Number=6, t=1mm	P6T1
	Number=4, t=2mm	P4T2
	Number=6, t=2mm	P6T2
X-plates	Plates Number=5, Thickness=1mm	XP5T1
	Number=7, t=1mm	XP7T1
	Number=5, t=2mm	XP5T2
	Number=7, t=2mm	XP7T2
Waves	Wave's width=5mm, Length=5mm	WW5L5
	W=5mm, L=7mm	WW5L7
	W=7mm, L=5mm	WW7L5
	W=7mm, L=7mm	WW7L7

Table 2. Example of weightage setting.

Criteria	Number of possible comparisons $N = n(n-1)/2 = 5(5-1)/2 = 10$										Score	Relative Weightage,
	1	2	3	4	5	6	7	8	9	10		
A	3	3	1	2							9	→ 9/40 = 0.225
B	1				2	3	1				7	→ 7/40 = 0.175
C		1			2			3	2		8	→ 8/40 = 0.200
D			3			1		1		1	6	→ 6/40 = 0.150
E				2			3		2	3	10	→ 10/40 = 0.250

4. Finite element model

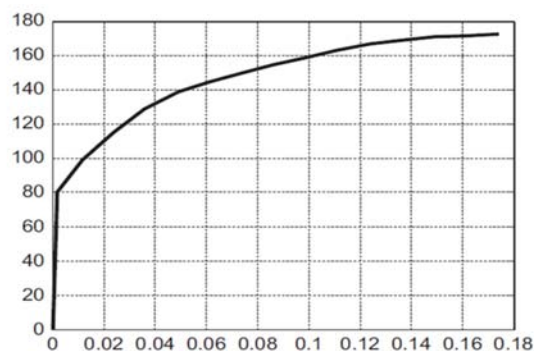
In this work the finite element model for the thin-walled tubular profiles were modelled using ABAQUS. The non-linear finite element code ABAQUS explicit was used to predict the response of the generated profiles after they were impacted by a striker. To model the profiles, a square cross section tube of 80x80 mm, 350 mm length and 2 mm thickness is considered. The thin walled tube was modelled using 4 node shell continuum (S4R) element of 2.5 mm size with reduced integration points. The top plate (striker) was modelled as a rigid body with a reference point mass of 275 kg and a predefined velocity field of 15.6 m/s. The striker's mass was selected to be 25% of an average sedan vehicle's mass (1100 kg). This was based on the fact that less than 50% of the vehicle's mass kinetic energy can be absorbed by two longitudinal tubes [32].

The striker's initial velocity was selected as 15.6 m/s (56 km/h) as the value used in National Car Assessment Program (NCAP) crash tests by the National Highway Traffic Safety Administration (NHTSA). The motion of the top plate was restricted to only translational motion along the tube's axes.

The thin-walled tube is fixed on the lower rigid plate using a constraint between their two surfaces. To account for the contact between the two plates and the tube, a general contact algorithm was chosen with a penalty coulomb friction coefficient of 0.2 [33]. This is to avoid the interpenetration between the tube walls. To model the design's profiles materials, the A-36 mild-steel model from [3] and AA6060T4 aluminum alloy model from [4] models were adopted. The adopted steel model is characterized by Johnson-Cook constitutive hardening model. The adopted steel model parameters are listed in Table 3. The AA6060T4 aluminum is characterized as an isotropic plastic material with the plastic behavior shown in Figure 7. The adopted aluminum model has a young modulus $E=68.21$ GPa, Poisson's ratio of 0.3 and yield strength $S_y = 80$ MPa. text.

Table 3. Johnson-Cook Parameters [3].

Parameters	Values
A	146.7 MPa
B	896.9 MPa
Strain Power Coefficient, N	0.32
C	0.033
Temperature Power Coefficient, M	0.323
Reference Strain Rate	1.0 s^{-1}
Density	7850 kg/m^3
Melting temperature, T_m	1773 K
Specific Heat, C_p	486 J/kg-K

**Figure 7.** Tensile test graph of AA6060T4 aluminum alloy [4].

5. Results and discussion

The energy absorption is plotted against the deformation length (Figure 8 (a) and (b)) for the highest energy absorbing profiles for steel and aluminum respectively. This is done to facilitate the comparison between the different profiles. The force-displacement diagrams for all of the tested profiles are shown in Figures 9–13. The following sub-sections includes a detailed explanation on the obtained crashworthiness parameters for the different generated concepts.

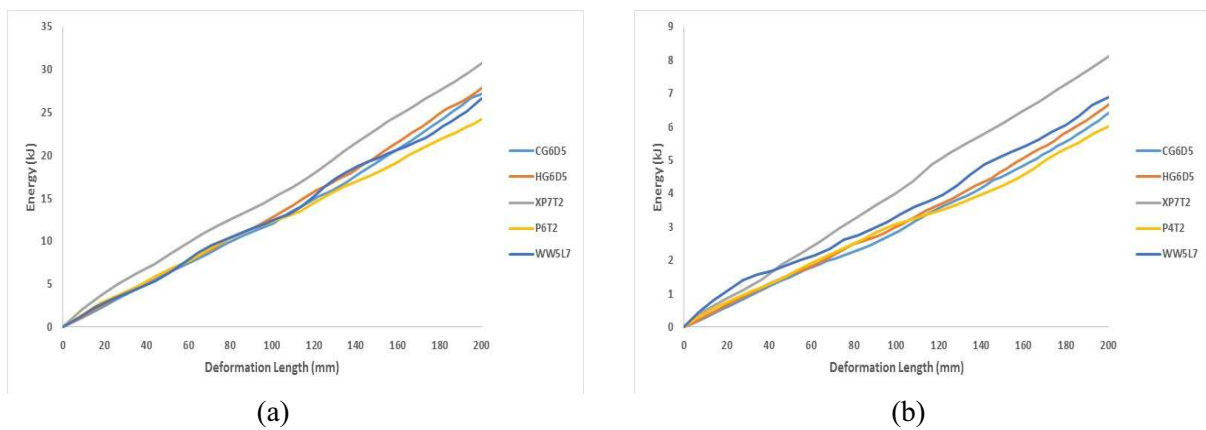


Figure 8. Energy against deformation length for best energy absorbing (a) steel (b) aluminium profiles

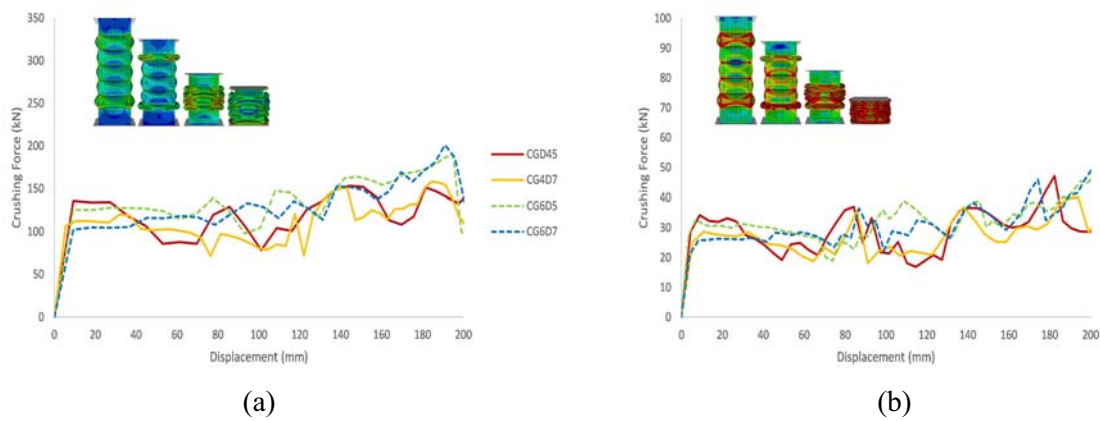


Figure 9. Force-displacement diagram for circular grooves profiles (a) steel (b) aluminium

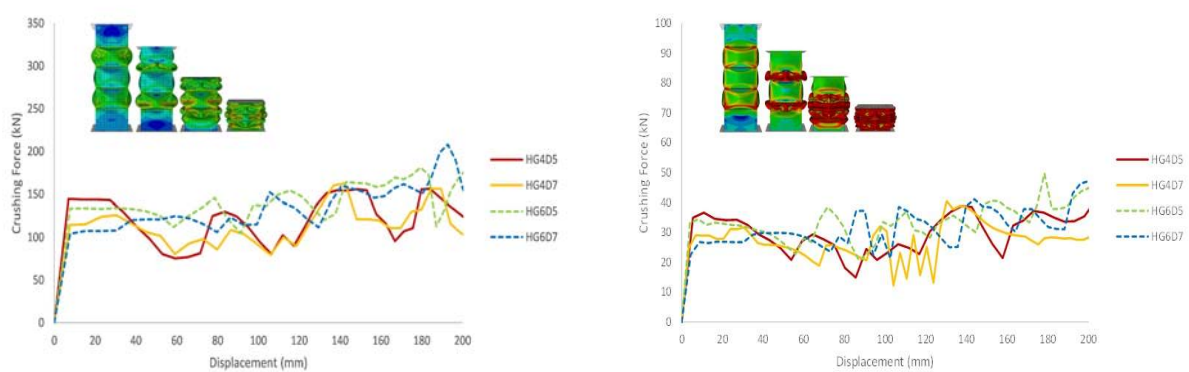


Figure 10. Force-displacement diagram for hexagonal grooves profiles (a) steel (b) aluminium

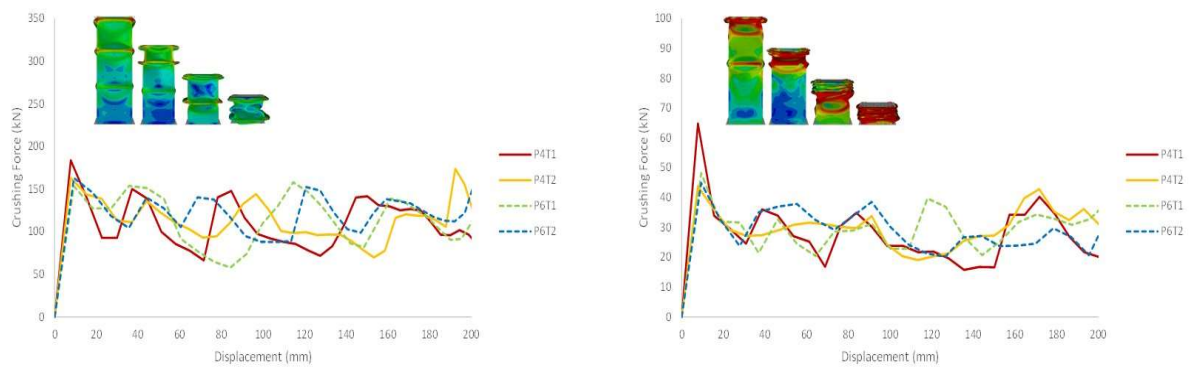


Figure 11. Force-displacement diagram for pyramid grooves profiles (a) steel (b) aluminium

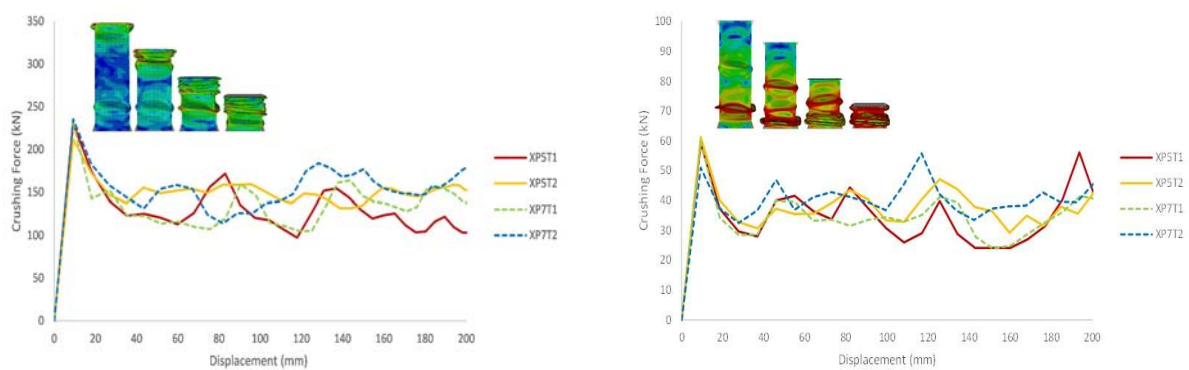


Figure 12. Force-displacement diagram for x-internal grooves profiles (a) steel (b) aluminium

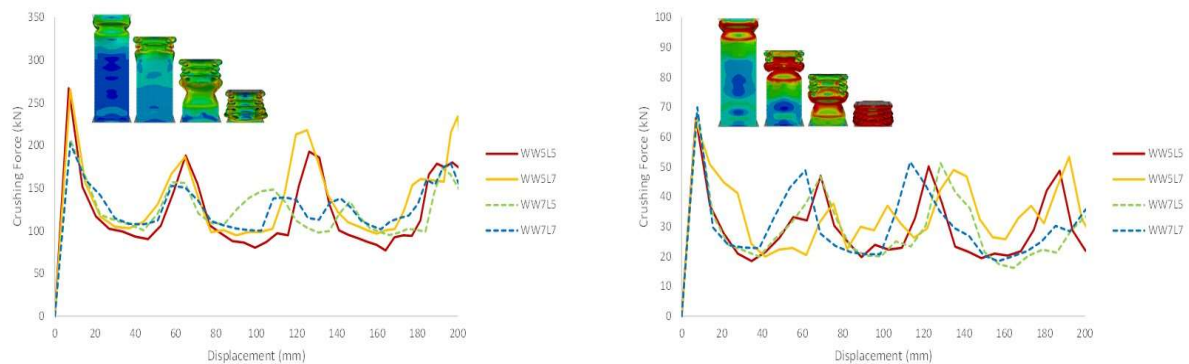


Figure 13. Force-displacement diagram for internal wavy sheets (a) steel (b) aluminium

The first step of the selection process is to choose the selection criteria. The main general principles that has to be achieved in an ideal energy absorber are: (1) restricted and constant reactive force, (2) light weight and high Specific Energy Absorption (SEA) and (3) low cost and easy installation [34]. To satisfy the first two principals, the following measured indicators were selected as evaluation criteria: the maximum crushing force (Pmax), Crushing Force Efficiency (CFE) and the Specific Energy Absorption (SEA). Similarly, the production criteria which assesses the complexity of the profile was selected to satisfy the last principle. The second step of the selection process is to determine the weight for each of the performance criteria. This is done using the Digital Logic method, in which two criteria are compared at a time. The details of this method have been explained previously. Tables 4 and 5 show the total score for each performance criteria for the steel and aluminum profiles respectively.

Table 4. Summary of the performance criteria scores for the steel-assigned profiles.

Model	CFE [%]	score	rating	SEA [J/kg]	score	rating	Pmax [kN]	score	rating	Production	rating	Total
CG4D5	84.7	9	2.97	24120.7	9	1.89	167.806	9	2.97	10	1.3	9.13
CG6D5	69.7	5	1.65	25658	9	1.89	189.419	7	2.31	8	1.04	6.89
CG4D7	85.1	9	2.97	23300.6	7	1.47	165.854	10	3.3	10	1.3	9.04
CG6D7	65	3	0.99	24273.2	9	1.89	201.188	6	1.98	7	0.91	5.77
HG4D5	88.6	10	3.3	24068.8	8	1.68	156.017	10	3.3	9	1.17	9.45
HG6D5	85	9	2.97	27154.2	10	2.1	181.138	8	2.64	7	0.91	8.62
HG4D7	87.3	10	3.3	23299.1	8	1.68	165.148	10	3.3	9	1.17	9.45
HG6D7	66.8	4	1.32	24831.1	8	1.68	214.405	5	1.65	8	1.04	5.69
P4T1	68.5	5	1.65	19863.1	5	1.05	183.717	8	2.64	2	0.26	5.6
P6T1	78.8	8	2.64	21278.1	6	1.26	159.834	10	3.3	1	0.13	7.33
P4T2	74.6	6	1.98	19773.5	5	1.05	173.887	9	2.97	2	0.26	6.26
P6T2	74	6	1.98	20985.6	6	1.26	182.951	8	2.64	1	0.13	6.01
XP5T1	58.3	1	0.33	21220.7	6	1.26	230.149	4	1.32	4	0.52	3.43
XP7T1	57.6	2	0.66	21783.9	6	1.26	231.409	4	1.32	3	0.39	3.63
XP5T2	68.9	5	1.65	21074.1	6	1.26	211.654	5	1.65	4	0.52	5.08
XP7T2	65.7	4	1.32	21633.2	6	1.26	235.354	3	0.99	3	0.39	3.96
WW5L5	58.4	2	0.66	15115.2	1	0.21	267.076	1	0.33	6	0.78	1.98
WW5L7	55	1	0.33	14041	1	0.21	265.562	1	0.33	6	0.78	1.65
WW7L5	73	6	1.98	15638.9	2	0.42	207.173	6	1.98	5	0.65	5.03
WW7L7	74.4	6	1.98	14941.6	1	0.21	202.397	6	1.98	5	0.65	4.82

It was found that the best steel profile is the hexagonal grooves (HG4D7), while the best aluminum profile is the circular grooves (CG4D7). Figure 14 illustrates the enhancements obtained for the maximum crushing force (Pmax), the crushing force efficiency (CFE) and the specific energy absorption (SEA) of the best selected profiles compared to the conventional empty steel and aluminum tubes. The selected steel profile (HG4D7) shows a reduction in (Pmax) of around 44 kN, an increase in (CFE) of around 30% and an increase in (SEA) of around 9 kJ/kg relative to the conventional empty steel tube tested in [3]. Similarly, the selected aluminum profile (CG4D7) shows a reduction in (Pmax) of around 85 kN, an increase in (CFE) of around 42% and an increase in (SEA) of around 10 kJ/kg compared to the conventional empty aluminum tube tested in [35].

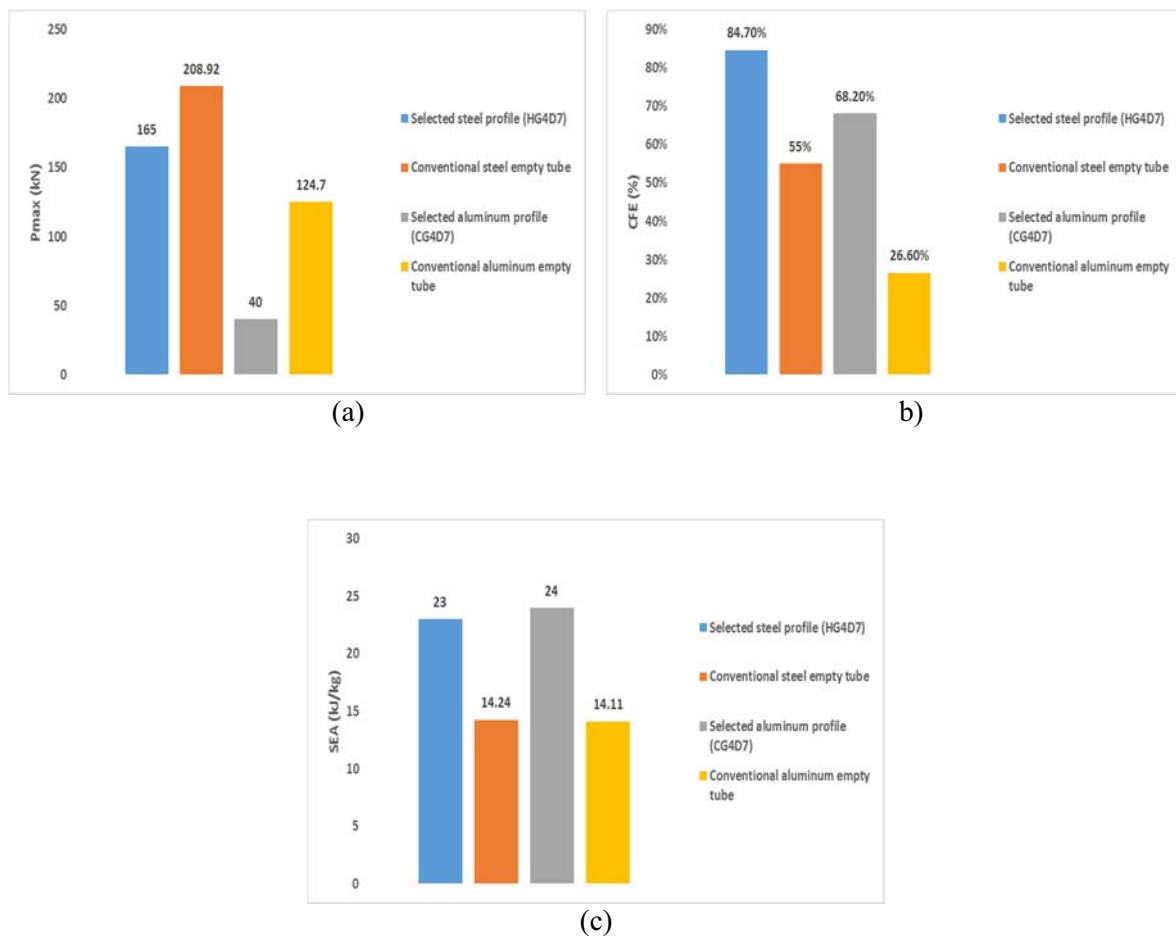


Figure 14. Comparison values for (a) peak force (b) crush force efficiency (c) specific energy

6. Conclusions

The crash response of different complex geometrical designs of steel and aluminum were examined numerically using ABAQUS software. The different complex-geometries designs parameters were altered which resulted in 20 profiles that were tested numerically for both steel and aluminum. All numerical tests were dynamics with speed of 15.6 m/s and an impact mass of 275 kg. Different crashworthiness indicators were obtained to assess the performance of the tested profiles. The indicators were then weighted according to their significance to select the most efficient crashworthy profile using a multi-criteria decision making process. It was found that the hexagonal grooves (HG4D7) profile was better for crashworthiness application than the other steel profiles, while the circular grooves (CG4D7) profile was better than the other aluminum profiles. The steel (HG4D7) profile had a maximum crushing force value of 165 kN, specific energy absorption value of 23 kJ/kg and crushing force efficiency of 87%. Similarly, the aluminum (CG4D7) profile had a maximum crushing force value of 40 kN, specific energy absorption value of 24 kJ/kg and crushing force efficiency of 68%. In conclusion, it can be stated that the best selected profiles (HG4D7) and (CG4D5) had enhanced the crashworthiness of the thin walled structure, showing the potential of using additive manufacturing techniques in automotive safety applications in the future. However, further experimental investigation is required to assure the accuracy of the numerical material's models.

Table 5. Summary of the performance criteria scores for the aluminum-assigned profiles.

Model	CFE [%]	score	rating	SEA [J/kg]	score	rating	Pmax [kN]	score	rating	Production	rating	Total
CG4D5	59.1	7	2.31	28463.7	8	1.68	47.135	8	2.64	10	1.3	7.93
CG6D5	67.3	10	3.3	28938.5	9	1.89	47.27	8	2.64	8	1.04	8.87
CG4D7	68.2	10	3.3	23928.3	6	1.26	40.066	10	3.3	10	1.3	9.16
CG6D7	61.9	8	2.64	32353.9	10	2.1	49.99	7	2.31	7	0.91	7.96
HG4D5	54.5	5	1.65	27165.7	8	1.68	54.254	6	1.98	9	1.17	6.48
HG6D5	60.5	8	2.64	28061	8	1.68	54.868	6	1.98	7	0.91	7.21
HG4D7	56.5	6	1.98	24809.1	7	1.47	50.378	7	2.31	9	1.17	6.93
HG6D7	65.5	9	2.97	25138.2	7	1.47	47.863	8	2.64	8	1.04	8.12
P4T1	42.2	1	0.33	15779.7	2	0.42	64.767	2	0.66	2	0.26	1.67
P6T1	51.2	4	1.32	23634.2	6	1.26	61.704	3	0.99	1	0.13	3.7
P4T2	66.5	9	2.97	15854.8	2	0.42	43.821	9	2.97	2	0.26	6.62
P6T2	66.2	9	2.97	20547.8	5	1.05	44.864	9	2.97	1	0.13	7.12
XP5T1	55.4	6	1.98	16905.8	3	0.63	59.249	4	1.32	4	0.52	4.45
XP7T1	54.6	5	1.65	16608.6	3	0.63	59.887	4	1.32	3	0.39	3.99
XP5T2	64.9	9	2.97	16955.7	3	0.63	61.315	3	0.99	4	0.52	5.11
XP7T2	69.8	9	2.97	20335	4	0.84	55.845	5	1.65	3	0.39	5.85
WW5L5	44.1	2	0.66	19349.5	4	0.84	66.338	2	0.66	6	0.78	2.94
WW5L7	49.9	4	1.32	18546.5	4	0.84	65.529	2	0.66	6	0.78	3.6
WW7L5	40.7	1	0.33	19688.6	4	0.84	68.01	1	0.33	5	0.65	2.15
WW7L7	43.6	1	0.33	12625.9	1	0.21	69.946	1	0.33	5	0.65	1.52

References

- [1] International Energy Agency (Retrieved on 11th April, 2016) Available from: <http://www.iea.org/>
- [2] The Global Status Report on Road Safety 2013 World Health Organization (WHO) Available from: www.who.int
- [3] Tarlochan F, Samer F, Hamouda A, Ramesh S and Khalid K 2013 *Thin-Walled Structures* **71** 7-17
- [4] Tang Z, Liu S and Zhang Z A 2013 *Thin-Walled Structures* **62** 75-84
- [5] Nia A and Parsapour M 2014 *Thin-Walled Structures* **74** 155-65
- [6] Zhang X, Wen Z and Zhang H 2014 *Thin-Walled Structures* **84** 263-74
- [7] Guangyao L, Fengxiang X, Guangyong S and Qing L 2015 *International Journal of Impact Engineering* **77** 68–83
- [8] Jianguang F, Yunkai G, Guangyong S, Gang Z and Qing L 2015 *International Journal of Mechanical Sciences* **103** 63–73
- [9] Shahi V and Marzbanrad J 2012 *Thin-Walled Structures* **60** 24-37
- [10] Smith D, Graciano C and Martínez G 2014 *Thin-Walled Structures* **84** 170-6
- [11] Smith D, Graciano C, Martínez G and Teixeira P 2014 *Thin-Walled Structures* **85** 42-9
- [12] Liu S, Tong Z, Tang Z, Liu Y and Zhang Z 2015 *Thin-Walled Structures* **88** 70-81
- [13] Reddy S, Abbasi M and Fard M 2015 *Thin-Walled Structures* **94** 56-66
- [14] Abbasi M, Reddy S, Ghafari-Nazari A and Fard M 2015 *Thin-Walled Structures* **89** 31-41
- [15] Sharifi S, Shakeri M, Fakhari H and Bodaghi M 2015 *Thin-Walled Structures* **89** 42-53
- [16] Abbas N, and Pourya H O 2016 *Thin-Walled Structures* **100** 113-23
- [17] Yin H, Wen G, Liu Z and Qing Q 2014 *Thin-Walled Structures* **75** 8-17
- [18] Ahmad Z, Thambiratnam D and Tan A 2010 *International Journal of Impact Engineering* **49** 475-88
- [19] Hanssen A, Langseth M and Hopperstad O 2001 *International Journal of Mechanical Sciences* **43** 153-76

- [20] Hanssen A, Langseth M and Hopperstad O 2000 *International Journal of Mechanical Sciences* **24** 347-83
- [21] Zhang X and Cheng G 2007 *International Journal of Impact Engineering* **34** 1739-52
- [22] Yin H, Wen G, Liu Z and Qing Q 2014 *Thin-Walled Structures* **75** 8-17
- [23] Djamaluddin F, Abdullah S, Ariffin A and Nopiah Z 2015 *Thin-Walled Structures* **87** 1-11
- [24] Goel M 2015 *Thin-Walled Structures* **90** 1-11
- [25] Qiang G, Liangmo W, Yuanlong W and Chenzhi W 2016 *Thin-Walled Structures* **100** 105-12
- [26] Sun G, Li G, Hou, S, Zhou S, Li W and Li Q 2010 *Materials Science and Engineering A* **527** 1911-9
- [27] Omid M and Hashem G 2016 *Thin-Walled Structures* **98** 627-39
- [28] Guangyao L, Zheshuo Z, Guangyong S, Fengxiang X and Xiaodong H 2014 *International Journal of Mechanical Sciences* **89** 439-52
- [29] Janguang F, Yunkai G, Guangyong S, Yuting Z, and Qing L 2014 *Computational Materials Science* **90** 265-75
- [30] Hanfeng Y, Guilin W, Hongbing F, Qixiang Q, Xiangzheng K, Juru X and Zhibo L 2014 *Materials and Design* **55** 747-57
- [31] Farag M M 2008 *Materials and Process Selection for Engineering Design* (Boca Raton: CRC Press)
- [32] Witteman W J 1999 *Improved vehicle crashworthiness design by control of the energy absorption for different collisions situation* (PhD thesis) Netherlands: Eindhoven University of Technology
- [33] Dehghan-Manshadi B, Mahmudi H, Abedian A and Mahmudi R 2007 *Materials & Design* **28** 8-15
- [34] Lu G and Yu T X 2003 *Energy absorption of structures and materials* (Boca Raton: CRC Press)
- [35] Cheng Q, Altenhof W and Li L 2006 *Thin-Walled Structures* **44** 441-54